An environmental ecocorona influences the formation and evolution of the biological corona on the surface of single-walled carbon nanotubes

Abdolahpur Monikh, F.; Chupani, L.; Karkossa, I.; Gardian, Z.; Arenas-Lago, D.; Bergen, M. von; ... ; Peijnenburg, W.J.G.M.
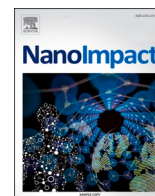
Research Paper

An environmental ecocorona influences the formation and evolution of the biological corona on the surface of single-walled carbon nanotubes

Fazel Abdolahpur Monikh [a,b,*], Latifeh Chupani [c], Isabel Karkossa [d], Zdenko Gardian [e], Daniel Arenas-Lago [i], Martin von Bergen [d,f], Kristin Schubert [d], Veronika Piackova [c], Eliska Zuskova [c], Wim Jiskoot [g], Martina G. Vijver [a], Willie J.G.M. Peijnenburg [a,h]

[a] *Institute of Environmental Sciences (CML), Leiden University, P.O. Box 9518, 2300, RA, Leiden, Netherlands*
[b] *Department of Environmental & Biological Sciences, University of Eastern Finland, P.O. Box 111, FI-80101 Joensuu, Finland*
[c] *University of South Bohemia in Ceske Budejovice, Faculty of Fisheries and Protection of Waters, South Bohemian Research Center of Aquaculture and Biodiversity of Hydrocenoses, Zátiší 728/II, 389 25 Vodňany, Czech Republic*
[d] *Department of Molecular Systems Biology, UFZ, Helmholtz-Centre for Environmental Research, Permoserstraße 15, 04318 Leipzig, Germany*
[e] *Institute of Parasitology, Biology Centre, Czech Academy of Sciences, University of South Bohemia, Faculty of Science, Branišovská 31, 370 05 České Budějovice, Czech Republic*
[f] *Institute of Biochemistry, Leipzig University, Permoserstraße 15, 04318 Leipzig, Germany*
[g] *Division of BioTherapeutics, Leiden University, Einsteinweg 55, 2333, CC, Leiden, the Netherlands*
[h] *National Institute of Public Health and the Environment (RIVM), Center for Safety of Substances and Products, Bilthoven, the Netherlands*
[i] *Department of Plant Biology and soil Science, University of Vigo, As Lagoas, Ourense, Spain*

ARTICLE INFO

ABSTRACT

Nanomaterials (NMs) taken up from the environment carry a complex ecocorona consisting of dissolved organic matter. An ecocorona is assumed to influence the interactions between NMs and endogenous biomolecules and consequently affects the formation of a biological corona (biocorona) and the biological fate of the NMs. This study shows that biomolecules in fish plasma attach immediately (within <5 min) to the surface of SWCNTs and the evolution of the biocorona is a size dependent phenomenon. Quantitative proteomics data revealed that the nanotube size also influences the plasma protein composition on the surface of SWCNTs. The presence of a pre-attached ecocorona on the surface of SWCNTs eliminated the influence of nanotube size on the formation and evolution of the biocorona. Over time, endogenous biomolecules from the plasma partially replaced the pre-attached ecocorona as measured using a fluorescently labelled ecocorona. The presence of an ecocorona offers a unique surface composition to each nanotube. This suggests that understanding the biological fate of NMs taken up from the environment by organisms to support the environmental risk assessment of NMs is a challenging task because each NM may have a unique surface composition in the body of an organism.

1. Introduction

Carbon nanotubes (CNTs), being miniscule (10^{-9} m) rolled up seamless cylinders of graphene sheets, are a promising category of nanomaterials (NMs) with a rapid expansion of applications ranging from development of electronic devices (Javey et al., 2003) to bio-sensors (Chen et al., 2003), and drug delivery systems (Pantarotto et al., 2004; Thakare et al., 2010). This broad application is due to their remarkable properties such as the hollow cavity, nanoscale size and their high volume specific surface area (De Volder et al., 2013). The toxicological, pharmacological, and environmental risk profiles of CNTs are increasingly being studied (Ge et al., 2011; Higgins et al., 2011; Lacerda et al., 2006) to reveal the behavior and toxicity of CNTs in biological systems.

It is well documented that NMs adsorb a mixture of biomolecules when they are in contact with physiological media. The biomolecules (such as proteins, carbohydrates, lipids, nucleic acids, and small molecules) adsorbed to NMs form a so-called biological corona (referred to as biocorona in this study) (Lynch et al., 2007; Mu et al., 2008), which determines the biological identity of NMs (Albanese et al., 2014; Gasser et al., 2010). The physicochemical properties of NMs, such as size and surface composition, and their exposure time in biological media can

---

influence the formation of such a biocorona (Mu et al., 2008; Tenzer et al., 2013; Zhang et al., 2011). This implies that each NM may have a unique fingerprint in terms of which biomolecules bind to the NM surface and become part of its biocorona (Chetwynd and Lynch, 2020). Acquisition of a biocorona significantly modulates the extrinsic physicochemical properties of NMs such as diameter, colloidal stability and surface charge. This, in turn, may affect the biological fate of NMs (Francia et al., 2019; Gunawan et al., 2014; Kumar et al., 2016; Monopoli et al., 2011; Mu et al., 2008; Nel et al., 2009) such as cellular uptake, biodistribution, biotransformation and clearance.

In case of a protein corona, it has been reported that some rearrangements of the corona take place in the first few hours of incubation in a physiological medium (Baimanov et al., 2019). The proteins with a low affinity which initially occupy the surface of the NMs are replaced by proteins of a high affinity (Baimanov et al., 2019; Cedervall et al., 2007; Lesniak et al., 2010). Eventually the corona composition will reach a steady-state (Lynch and Dawson, 2008). Nevertheless, the understanding of the formation of a dynamic biocorona on the surface of NMs is limited (Gasser et al., 2010). The formation and the composition of a biocorona on the surface of NMs potentially depend not only on the composition of the medium in which the NMs are currently residing, but also on the history of pre-exposure of NMs in other environments. So, pre-attachment of any molecule on the surface of NMs may modulate the formation and evolution of a biocorona (Perng et al., 2019). It was, for example, documented that pre-coating of CNTs with surfactants (Gasser et al., 2010) and proteins (Saptarshi et al., 2013) influences the subsequent adsorption of plasma proteins on the surface of the nanotubes, as observed also for silica and polystyrene NMs (Du et al., 2019; Lundqvist et al., 2011; Perng et al., 2019).

Previous studies showed that NMs in the environment adsorb natural organic matter (NOM) (Xu et al., 2020; Yang and Xing, 2009) on their surface to form a so-called ecological corona (ecocorona) (Fadare et al., 2020; Hyung et al., 2007). NOM consists of a heterogeneous mixture of biomolecules resulting mostly from the degradation of organisms in the environment, such as hydrophilic acids, proteins, lipids, carbohydrates, carboxylic acids, amino acids, etc. The ecocorona modifies the surface of CNTs and determines the environmental identity of CNTs before entering biota. To date, it remains unknown how the presence of an ecocorona on the surface of CNTs influences the formation, evolution, and composition of the biocorona when the CNTs are taken up by organisms.

Herein, we studied how pre-attachment of an ecocorona on single-walled CNTs (SWCNTs) of two different sizes influences the time-resolved formation and composition of a biocorona on the surface of the nanotubes. Accordingly, SWCNTs of two different sizes were incubated in a dissolved organic matter (DOM) solution for 24 h followed by incubation in fish plasma (carp) for varying periods of time. The interactions between the pre-attached ecocorona and the biomolecules of the plasma resulted in the formation of a corona consisting of a mixture of an ecocorona and a biocorona (bio-ecocorona-SWCNTs complexes). We demonstrate that the presence of an ecocorona influences the thickness and the surface charge of the bio-ecocorona-SWCNTs regardless of nanotube size. We measured the thickness of the corona on the surface of SWCNTs and we are not sure if this corona is solely made of proteins, thus we refer to this corona as biocorona throughout the study. In some cases, where we only determined the protein part of this corona, we refer to that as protein corona. By fluorescently labelling the ecocorona, we revealed that the replacement of the ecocorona by a biocorona is time and size dependent, but a complete replacement does not occur within the 25 h exposure duration applied. By using quantitative proteomics, we demonstrated that the SWCNT size and the presence of an ecocorona influence the quantity and type of proteins contributing to the formation of the biocorona.

2. Materials and methods

2.1. Materials

A Millipore Milli-Q (MQ) system was used to provide the MQ water for the experiment. The SWCNTs were purchased from Sigma Aldrich (St. Louis, USA) with diameter × medium length of 0.75 nm × 3 µm (SWCNT-1) and 0.83 nm × 1 µm (SWCNT-2). Suwannee River NOM was purchased from the International Humic Substances Society (1R101N). Sodium dodecyl sulfate (SDS), ammonium bicarbonate, triethylammonium bicarbonate buffer (TEAB), tris(2-carboxyethyl)phosphine, hydroxylamine and dimethyl sulfoxide were purchased from Sigma Aldrich, Germany. Iodoacetamide, acetonitrile and ethanol were supplied by Merck (Germany). Trypsin was purchased from Promega, USA. The TMT10plex™ Isobaric Label Reagent Set was supplied by Thermo Scientific, USA. Ammonium formate was purchased from Agilent Technologies, USA. The fluorescence material, 5-DTAF (5-(4,6-dichlorotriazinyl) aminofluorescein), was purchased from ThermoFischer Scientific.

2.2. Preparation of fish plasma

The blood was collected from a caudal vein of juvenile common carp (*Cyprinus carpio* L.), strain of Ropsha scaly, using a heparinized syringe. Plasma was separated by centrifuging at 4 °C/10 min/4000 RPM and immediately snap frozen in liquid nitrogen. Fish were raised under laboratory conditions from larval stage until juvenile stage.

2.3. Preparation of SWCNTs dispersion in phosphate-buffered saline

Dispersions of the SWCNT1–1 and SWCNT-2 were prepared in phosphate-buffered saline (PBS, 0.1 M and pH 7.5 was used in all experiments unless otherwise mentioned) to reach a final concentration of 1 g L^{-1} of SWCNTs. The dispersions were sonicated using a bath sonicator (35 kHz frequency, DT 255, Bandelin electronic, Sonorex digital, Berlin, Germany) in an ice bath for 5 min. The time of sonication was optimized to reach a time point at which the sonication process did not break down the tubes. The SWCNTs aggregated within 1 min after sonication, which made characterization of the SWCNTs in PBS dispersion not feasible in this study. Therefore, for imaging and comparison purposes, the SWCNTs were dispersed in 1% SDS solution followed by 5 min bath sonication.

2.4. Characterization of SWCNTs

Transmission electron microscopy (TEM, JEM-1400, the Netherlands) was used to determine the size, shape and agglomeration profile of the SWCNT. To be able to provide TEM images of a single tube of SWCNTs, the SWCNTs were dispersed in 1% SDS solution followed by 5 min bath sonication in an ice bath. These dimensions of the SWCNTs were determined from TEM images, 600 nanotubes were counted. The ζ-potential was measured based on Laser Doppler electrophoresis using a Zetasizer Nano ZS (Malvern Instruments). The specific surface areas were measured according to the classical method of Brunauer–Emmett–Teller (BET) by nitrogen adsorption/desorption at 77 K using a Micromeritics Flowsorb 2300 (Norcross, USA).

2.5. Incubation of SWCNTs in DOM solution: formation of ecocorona

The procedures for preparing the DOM solution is reported in S1, Supplementary Information. To allow for the formation of an ecocorona on the surface of the SWCNTs, the NOM solution was filtered through a 0.45 µm Whatman filter paper to obtain the DOM (Arenas-Lago et al., 2019) and remove the insoluble NOM, which may facilitate isolation of the SWCNTs from the dispersion phase (see Supplementary Information, Fig. S1c). Stock dispersions of 100 mg L^{-1} of the SWCNTs were prepared

in 40 mg L^{-1} of DOM solution and sonicated for 5 min in a bath sonicator. Aliquots of the dispersion were used immediately after sonication for further experiments and the rest of the dispersions were incubated for 24 h. The formation of DOM ecocorona on the surface of the SWCNTs was investigated for both 5 min and 24 h incubation.

2.6. Incubation of the SWCNT in fish plasma

The dispersions of SWCNTs in PBS (100 mg L^{-1}) were incubated in fish plasma to reach a final concentration of 50 mg L^{-1} SWCNTs in 1 fold diluted plasma. The 50 mg L^{-1} concentration of the SWCNTs was arbitrarily selected to facilitate the SWCNTs characterization and protein corona measurement in the following experiments. The samples were put on a rotator at 4 °C and incubated for different time points of 5 min, 1 h, 6 h and 24 h. After each incubation time, the unbound proteins were removed by a stepwise washing process: i) 1 mL of PBS was added to the sample and centrifuged at 2500 $\times g$ and 4 °C for 10 min, ii) the supernatant was removed, and the previous washing step was repeated twice and, iii) 1 mL NH$_4$HCO$_3$ was added to the resulting pellets. The sample were stored at −80 °C for further analysis. Four replicates were prepared for each time point.

2.7. Incubation of ecocorona-SWCNTs in fish plasma

After 24 h incubationb of SWCNTs with 40 mg L^{-1} DOM, the dispersions were centrifuged at 5000 g for 10 min at 4 °C (Sorvall RC5Bplus centrifuge, Fiberlite F21–8) and the pellets, which contained the DOM-coated SWCNTs, were separated. The pellets were dispersed in PBS and incubated in the fish plasma. Accordingly, 200 μL of the ecocorona-SWCNTs were added to 200 μL of fish plasma and incubated on a rotator at 4 °C for different time points, including 5 min, 1 h, 6 h and 24 h. Subsequently, the unbound proteins were removed by the washing process described in the previous section (Incubation of the SWCNT in fish plasma) and the samples were stored at −80 °C for further analysis.

2.8. Observation of corona-SWCNT

TEM was applied to observe the formation of biocorona, ecocorona and bio-ecocorona on the surface of the SWCNTs. The specimens were placed on glow-discharged carbon-coated copper grids and negatively stained with 1.2% uranyl acetate, visualized by a JEOL JEM-2100F TEM (Japan, using 200 kV). The TEM images were recorded with a bottom-mount GatanCCD Orius SC1000 camera. The average thinness of the corona on the surface of the SWCNTs was measure by using the ImageJ software.

2.9. Testing the affinity of ecocorona and biocorona for the surface of SWCNTs

To test whether the biocorona can totally or partially replace the ecocorona on the surface of the SWCNTs, we first labelled the DOM using fluorescent material, 5-DTAF (see Supplementary Information, S3). The SWCNTs (100 mg L^{-1}) were incubated with the fluorescently labelled DOM (40 mg L^{-1}) for different time points (5 min, 1 h, 6 h and 24 h). The hypothesis was that the labelled DOM attaches to the surface of the SWCNT over time. Thus, due to centrifugation, the concentration of the DOM in the supernatant decreases by assuming that the SWCNTs undergo sedimentation. After each incubation time, the samples were centrifuged at 5000 g for 10 min at 4 °C and the fluorescence intensity was measured over time using a Fluorescent spectrometer F900 (Edinburgh Instruments Ltd., UK) at excitation and emission maxima of ~492 and 516 nm, respectively.

After 24 h of SWCNTs incubation (100 mg L^{-1}) with 40 mg L^{-1} of the fluorescently labelled DOM, the dispersions were centrifuged and the pellets were separated. The pellets were dispersed in 5 mL of PBS and immediately incubated in the fish plasma. Accordingly, 500 μL of the

labelled DOM-coated SWCNTs were added to 500 μL of fish plasma and incubated on a rotator at 4 °C for different time points, including 5 min, 1 h, 6 h and 24 h. After each incubation time, the samples were centrifuged at 5000 g for 10 min at 4 °C and the fluorescence intensity was measured in the supernatant.

2.10. Preparation of protein corona samples with tandem mass tags for liquid chromatography tandem mass spectrometry and subsequent analyses

All conditions were analyzed in quadruplicates. The proteins were eluted from the SWCNTs as described earlier (Simon et al., 2018) with minor adjustments. In brief, a final concentration of 2% (v/v) SDS in 100 mM ammonium bicarbonate (pH 8) was used, followed by an incubation at 95 °C for 15 min. Afterwards, the samples were centrifuged at 20000 g for 1 h at room temperature and the protein amounts of the supernatants were determined using the Pierce™ BCA Protein Assay Kit (Thermo Scientific, USA). For each sample, 25 μg protein were further processed using paramagnetic beads that allow for single-pot sample processing (Hughes et al., 2018). The workflow was conducted as described before (Bannuscher et al., 2019) (See Supplementary Information, S4).

The liquid chromatography tandem mass spectrometry (LC-MS/MS) analysis was conducted as described earlier (Karkossa et al., 2019) with some adjustments. Samples were analyzed on a nano-UPLC system (Ultimate 3000, Dionex, USA). After trapping (Acclaim PepMap 100 C18, 3 μm, nanoViper, 75 μm × 5 cm, Thermo Fisher, Germany) at 5 μL/min, peptides were separated on a reversed-phase column (Acclaim PepMap 100 C18, 3 μm, nanoViper, 75 μm × 25 cm, Thermo Fisher, Germany), applying a non-linear gradient of 150 min at 0.3 μL/min. After separation, peptides were ionized using a chip-based ESI source (Nanomate, Advion, USA) and subsequently entered the mass spectrometer (QExactive HF, Thermo Scientific, USA) (See Supplementary Information, S4).

2.11. Statistical analysis

Results were analyzed statistically using SPSS version 23.0. The normality test was performed using a Kolmogorov–Smirnov test. One-way analysis of variance (ANOVA), followed by Duncan's post hoc test, was performed to determine statistically significant differences between samples with more than two variables. A paired Student's t-test was performed to compare between samples with two variables. To unravel significant changes compared to the fish plasma, a Student's t-test with subsequent Benjamini & Hochberg adjustment was performed. Furthermore, the top ten most enriched proteins over all time points were identified for each condition.

3. Results

We used SWCNTs of two different sizes, SWCNT-1 and SWCNT-2. TEM images (Supplementary Information, Fig. S1a) report detailed information regarding the morphology and size of each of the differently sized SWCNTs dispersed in 0.01 M PBS (pH 7.5). Both SWCNTs tended to agglomerate into bundles when dispersed in PBS (average of observing 600 nanotubes). The presence of these agglomerates prohibited us to measure the ζ-potential of the nanotubes in PBS. To measure the size distribution of the SWCNTs, the NMs were dispersed in 1% SDS solution. The data were plotted as frequency histograms to determine the mean length and diameter of the SWCNTs (Supplementary Information, Fig. S2). The SDS solution (1%) could not stabilize the particles for a long time after sonication. The specific surface area was >820 ± 80 m^2 g^{-1} for SWCNT-1 and > 700 ± 62 m^2 g^{-1} for SWCNT-2.

A schematic depiction of the attachment and evolution of ecocorona on the surface of nanotube walls after 5 min and 24 h of incubation time is provided in Fig. 1a. After the incubation of SWCNTs in a suspension of
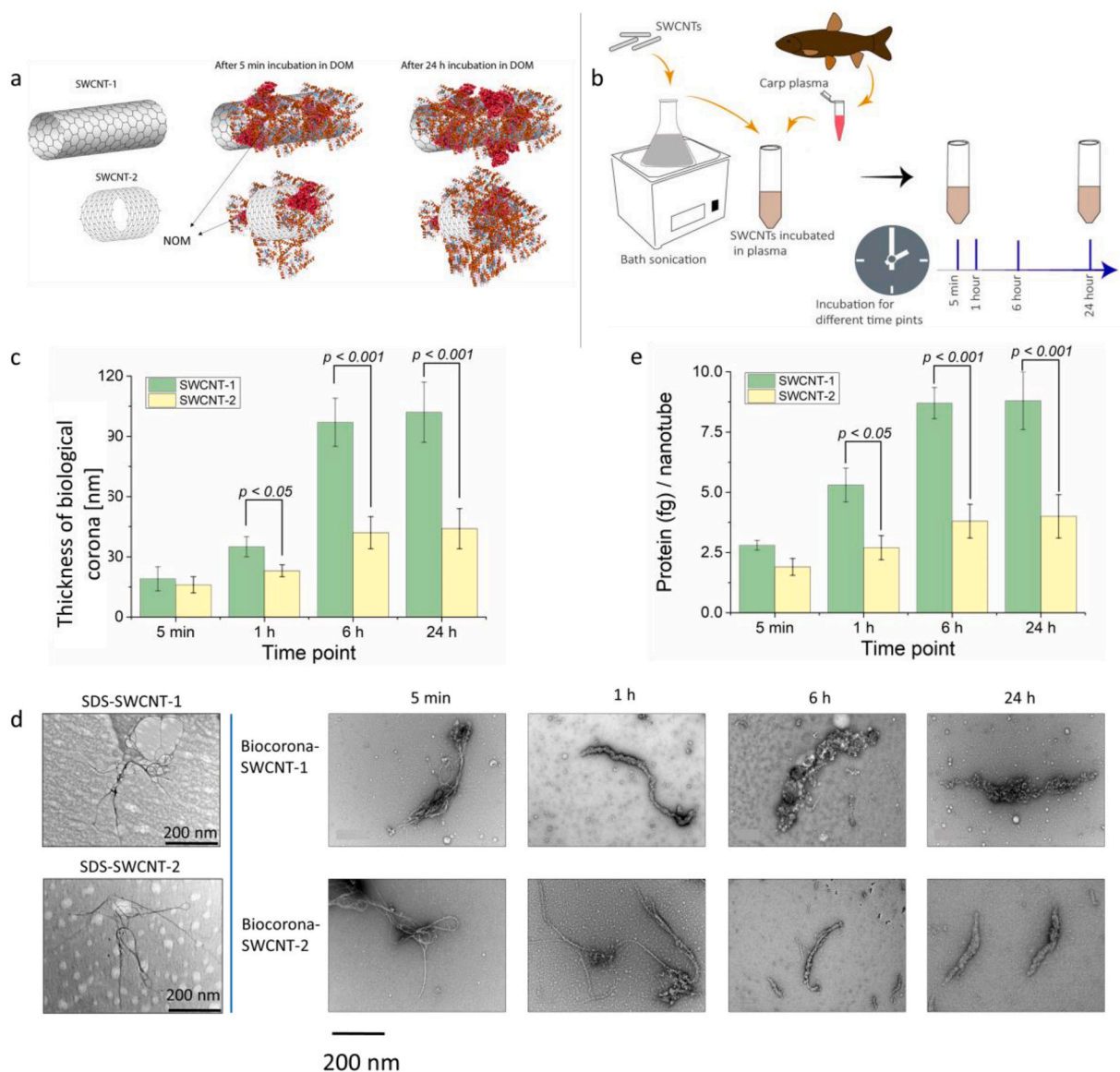
Fig. 1. a) Scheme of the incubation of SWCNTs in a suspension of dissolved organic matter (DOM). The brown molecules on the surface of the SWCNTs represent the DOM. b) Scheme of the incubation of SWCNTs with fish plasma. c) It shows the thickness of the biocorona-SWCNT complexes, which was measured (mean and SD of 100 tubes) using transmission electron microscopy (TEM). d) The TEM pictures were provided for dispersions of SWCNTs in 1% sodium dodecyl sulfate solution before incubation in plasma. For both SWCNTs, the biocorona increased the thickness with incubation time. e) Biological corona quantification by using protein as proxy. The figure shows the quantification of plasma proteins [femtogram (fg) per nanotube] at the indicated time points (values are mean ± SD).

40 mg L^{-1} of DOM (an environmentally relevant concentration (Abdolahpur Monikh et al., 2018)) for 5 min, the DOM ecocorona formed immediately on the surface of the tubes (Supplementary Information, Fig. S1b). The formed ecocorona offered a highly negative ζ-potential to the SWCNTs (Supplementary Information, Table S1) and acted as a stabilizer that increased the colloidal stability of the nanotubes in the dispersion, as measured by the number of single nanotubes in suspension (Supplementary Information, Fig. S2). Incubation of SWCNTs with 40 mg L^{-1} of DOM for 24 h significantly ($p < 0.05$) increased the absolute values of the ζ-potential. This finding confirmed our hypothesis on the increase of the amount of DOM adsorbed over time on the surface of SWCNTs (Supplementary Information, Table S1).

To allow formation of a biocorona, the SWCNTs were incubated in fish plasma obtained from carp with a concentration of 45 g L^{-1} proteins for 5 min, 1 h, 6 h and 24 h (Fig. 1b). Formation of a biocorona on the surface of the SWCNTs increased the absolute value of the negative ζ-potential from −5 to −28 mV for SWCNT-1 and from −4 to −29 mV for

SWCNT-2 following extension of exposure from 5 min to 6 h. Eventually, the ζ-potential reached a steady state at 6 h for both sizes (Supplementary Information, Tables S1). The biocorona also led to colloidal stabilization of the SWCNTs, i.e. the biocorona stabilized them against further agglomeration as measured by the size distribution of the tubes (Supplementary Information, Fig. S2). Consistent with the increase of the negative ζ-potential over time, the average thickness of the biocorona-SWCNT complexes increased significantly, as measured using TEM (Fig. 1c), until it reached a value of ~100 ± 12 nm for biocorona-SWCNT-1 and ~ 40 ± 8 nm for biocorona-SWCNT-2 after incubation for 6 h (Fig. 1c).

After 1, 6, and 24 h of incubation, the biocorona-SWCNT-1 was on average significantly ($p < 0.05$) thicker compared to the biocorona-SWCNT-2 (Fig. 1c). The TEM images (Fig. 1d) illustrate the increase in the thickness of the complexes over time. To facilitate the comparison between the size of SWCNTs with and without corona, we stabilized the SWCNTs using 1% SDS in MQ water. It is likely that the higher aspect

ratio of SWCNT-1 (aspect ratio of 4) compared to the SWCNT-2 (aspect ratio of 1.2) led to adsorption of a higher amount of biomolecules before reaching steady state, which in turn increased the thickness of the biocorona-SWCNT-1 complexes. To test this hypothesis, we quantified the total amount of proteins as proxy of the entire biocorona on the surface of the SWCNTs and normalized the values by the number of nanotubes in each treatment (see Supplementary Information S5). The results confirmed that a significantly higher amount of proteins (femtogram per nanotube) was attached to the surface of each tube of SWCNT-1 compared to the individual tubes of SWCNT-2 at 1 h, 6 h, and 24 h (Fig. 1e).

We incubated the DOM-coated SWCNTs (ecocorona-SWCNT complexes) in full fish plasma and allowed the interplay between the pre-attached ecocorona and the biomolecules of fish plasma for different time points: 5 min, 1 h, 6 h and 24 h. Four possibilities can be expected as a result of ecocorona and biocorona interaction: (a) the biocorona may partially replace the ecocorona, (b) the biocorona entirely replaces the ecocorona, (c) the biocorona forms on top of the ecocorona, or (d) the ecocorona entirely prevents formation of a biocorona (the SWCNTs are only covered by DOM). First, we determined the physicochemical properties of the complexes of biocorona-ecocorona-SWCNTs (referred to as bio-ecocorona-SWCNTs in this study) over time. The ζ-potential was roughly stable for the bio-ecocorona-SWCNT-2 (at ~ -23 mV) and its magnitude increased significantly ($p < 0.05$) for the bio-ecocorona-SWCNT-1 (from -23 to -38 mV) over time (Supplementary Information Table S2). The negative ζ-potential for the bio-ecocorona-SWCNT-1 increased (from -28 to -38 mV) and decreased for the bio-ecocorona-SWCNT-2 (from -29 to -23 mV) in magnitude at 24 h compared to the biocorona-SWCNTs without ecocorona at the same time point.

At time point 5 min, the bio-ecocorona-SWCNT-1 was thicker and at

the time point 6 h was thinner than the biocorona-SWCNT-1 at the same time points. The bio-ecocorona-SWCNT-2 was thicker at 1 h and 24 h than the biocorona-SWCNT-2 at the same time point. Interestingly, the thickness of the bio-ecocorona on the surfaces of both SWCNTs followed a similar temporal evolution (Fig. 2a). When we compared the two SWCNTs with each other, we identified minor differences between the thicknesses of the bio-ecocorona formed on the two SWCNTs (Fig. 2a). This suggests that the presence of a pre-attached ecocorona may determine the thickness of the bio-ecocorona on the surface of SWCNTs regardless of the size of the pristine nanotube. The temporal variation of the bio-ecocorona on the surface of both SWCNTs was pictured using TEM, as illustrated in Fig. 2b. The influence of the ecocorona on the quantity of the adsorbed proteins on the SWCNTs is shown in Fig. 2c. The presence of the ecocorona decreased the total quantity of attached proteins on both SWCNTs compared with the results obtained for biocorona-SWCNTs. The reduction in the quantity of the proteins due to the presence of an ecocorona was more pronounced for SWCNT-2.

It is possible that the ecocorona has a higher affinity to the surface of the SWCNTs compared to the biocorona, which would limit the partial or total replacement of the ecocorona by the biocorona. We tested this hypothesis for both SWCNTs by labelling the ecocorona before incubation with SWCNTs. As illustrated in Fig. 3a-e, the DOM molecules were dyed with 5-DTAF (5-(4,6-dichlorotriazinyl) aminofluorescein) (see S7, Supplementary Information), which is reported to label proteins and react directly with polysaccharides and other alcohols in aqueous solution (Helbert et al., 2003; Krahn et al., 2006), making the dye suitable for labelling DOM molecules. Based on the properties of the 5-DTAF, we expect that the label could be applied for humic acid and fulvic acid. We used the total DOM solution because it is representative of the real conditions of natural aquatic systems. The absorption of light by the
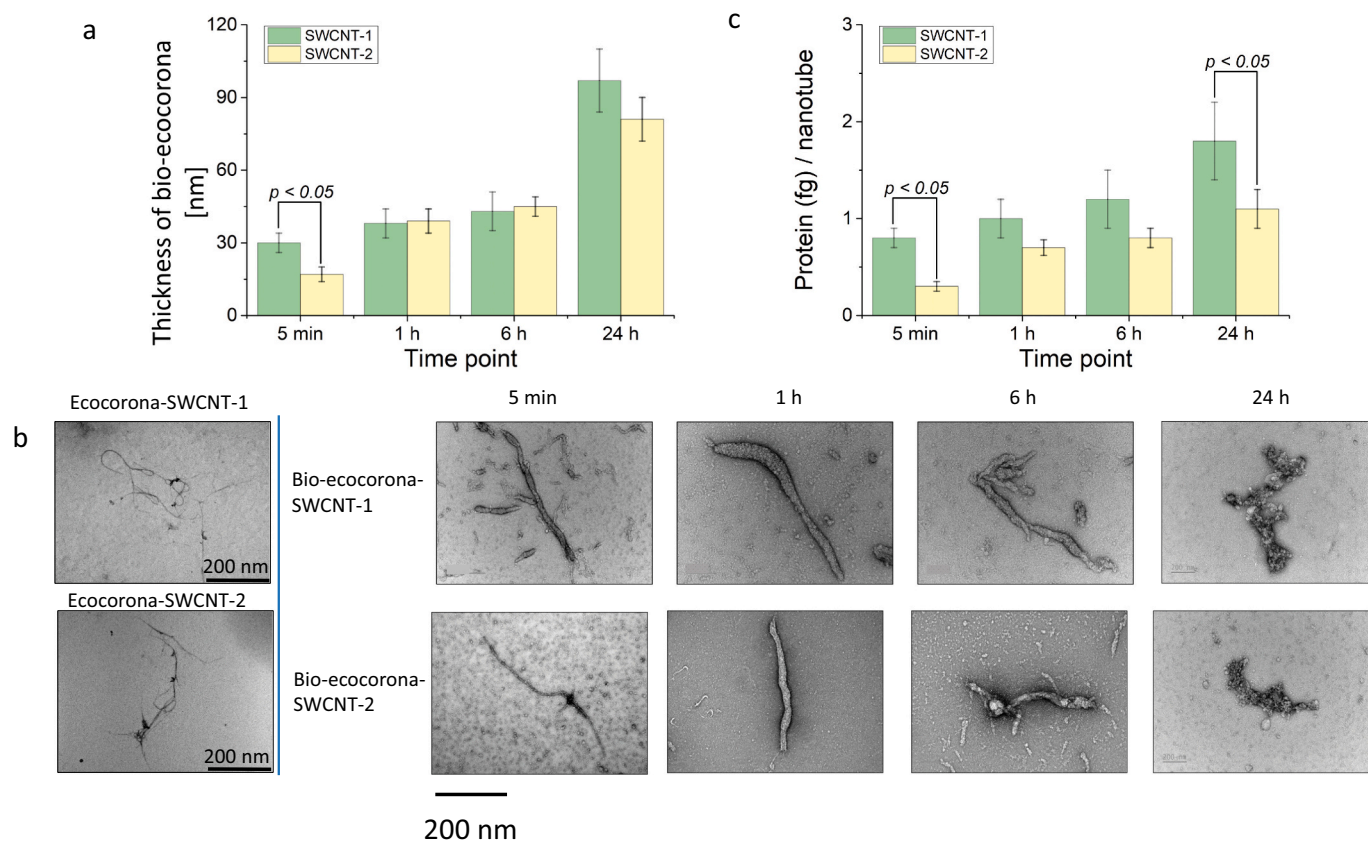
Fig. 2. a) Thickness of bio-ecocorona-SWCNT complexes, which was measured using TEM (mean ± SD, 100 complex) over time. b) TEM images showing the evolution and structure of the bio-ecocorona formed on the surface of the SWCNTs. c) Biocorona quantification by using the plasma proteins as proxies. The mass of the proteins on the surface of the SWCNTs (femtogram per nanotube) was measured at the indicated time points.
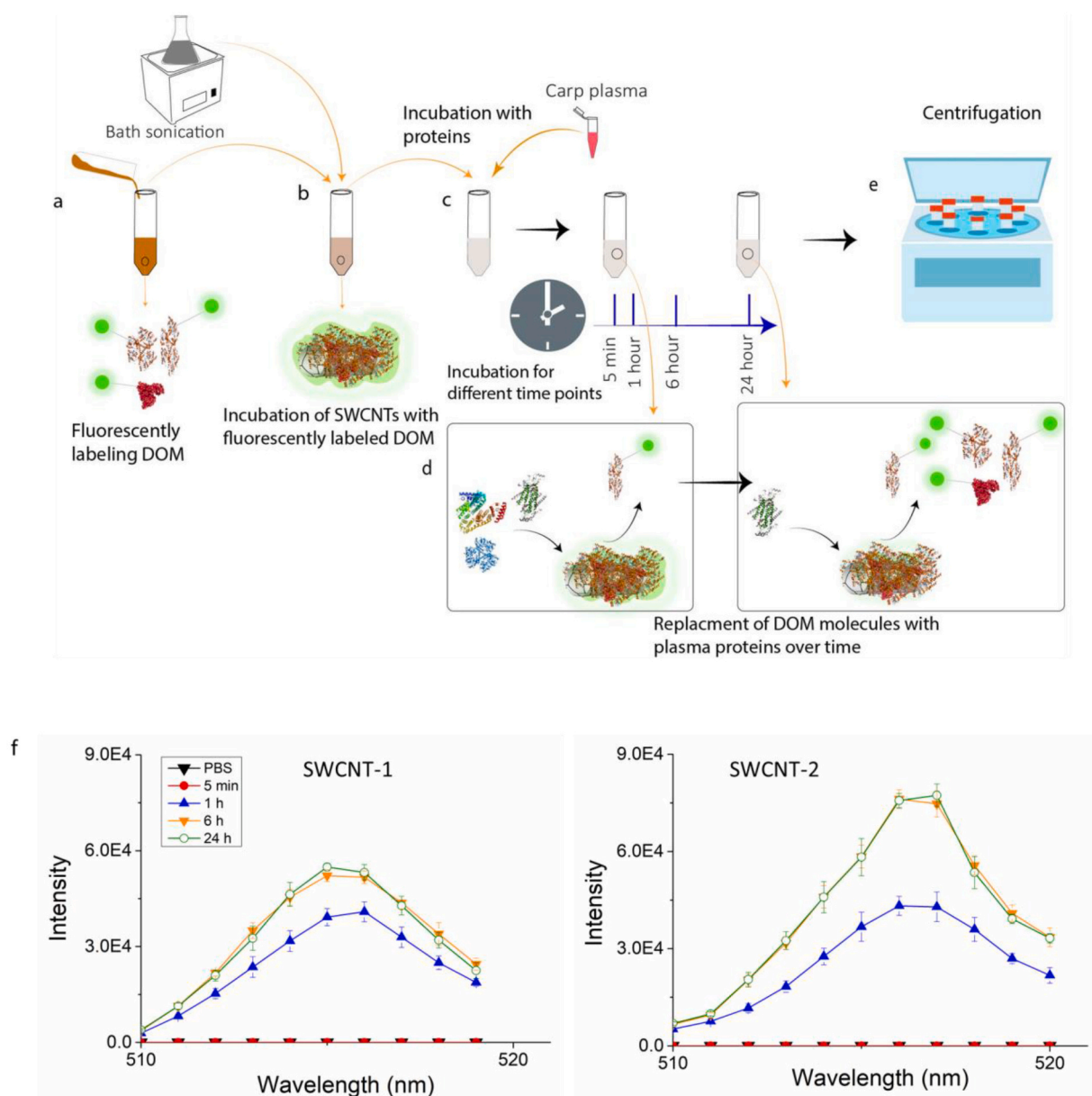
Fig. 3. a-e) Scheme of incubation of the SWCNTs with fluorescently labelled DOM and fish plasma is depicted: a) The DOM molecules were fluorescently labelled using 5-DTAF. b) The SWCNTs were incubated in the suspension of the fluorescently labelled DOM for 24 h. After 24 h, the SWCNTs and their labelled ecocorona were separated from the suspension of the fluorescently labelled DOM using centrifugation. c) The separated SWCNTs and their fluorescently labelled ecocorona were incubated in fish plasma for 5 min, 1 h, 6 h and 24 h. d) It is likely that the biomolecules of the plasma replaced the fluorescently labelled DOM over time. e) After each incubation time, the dispersion was centrifuged and the fluorescence intensity in the supernatant was measured. f) The measured emission spectra excited at ~492 nm. Data are shown as the mean ± SD of four independent experiments ($n = 4$).

labelled DOM was recorded by UV–Vis absorption spectroscopy (see the Supporting Information S3). The SWCNTs were incubated jointly with the labelled DOM for 24 h (Fig. 3b). After 24 h incubation, the labelled DOM-SWCNTs were separated using centrifugation and incubated with plasma (Fig. 3c, see S7 of Supplementary Information). Fig. 3d illustrates hypothetical interplays between the labelled ecocorona and the biocorona on the surface of the SWCNTs, showing the partial replacement of labelled DOM on the surface of SWCNTs by biomolecules. The signal of the fluorescence intensity at the emission maximum in the supernatant increased significantly after 1 h of incubation for both SWCNTs (area under the peak is 199,048 for SWCNT-1 and 211,424 for SWCNT-2) (Fig. 3f). By comparing these data with the control, where the labelled-ecocorona-SWCNTs were incubated in PBS (not in the plasma, see S7 of Supplementary Information), we could confirm that a fraction

of the DOM molecules on the surface of the SWCNTs was replaced with biomolecules of the plasma. At 6 h and 24 h, the fluorescence intensity of the dispersion of SWCNT-2 (area under the peak is 365,763 at 6 h and 361,887 at 24 h) was significantly ($p < 0.05$) higher than the fluorescence intensity of the SWCNT-1 (area under the peak is 272,216 at 6 h and 268,788 at 24 h) dispersion. This suggests that the ecocorona replacement in case of SWCNT-2 is higher.

Finally, we identified the bio-ecocorona on the surface of the SWCNTs using untargeted proteomics to provide insights into the composition of the protein corona over time. As mentioned earlier, DOM contains many different biological molecules, which makes the identification of the entire bio-ecocorona challenging. The biocorona alone consists of proteins and other biomolecules of the plasma. Herein, for simplicity, we only focus further on the protein corona as a proxy of the

entire bio-ecocorona. Accordingly, we applied a proteomic approach to get insight into the protein corona composition with respect to different sizes of SWCNTs and the presence/absence of the ecocorona at different time points. The protein corona on the surface of SWCNTs was eluted and subsequently identified and quantified using LC-MS/MS.

We examined Log2-transformed fold changes (FCs) of the abundances of plasma proteins bound to the SWCNTs relative to their respective abundances in the pure plasma. A principal component analysis (PCA) of the obtained Log2(FCs) was used to identify overall differences in the protein corona composition under the investigated conditions (Fig. 4a). A clear difference between the Log2(FCs) of the protein coronas formed on the surfaces of SWCNT-1 and SWCNT-2 was observable, as indicated by the full separation in the performed PCA. Interestingly, in the presence of the ecocorona, a separation was observable for the protein corona formed on SWCNT-1 but not on SWCNT-2. The PCAs of Log2(FCs) at the four investigated time points (Fig. 4b) revealed only minor differences between the time points (Fig. 4b). For SWCNT-1 with ecocorona, the first two time points were distinguishable from the last two, while in case of SWCNT-2 with ecocorona only the second time point was separated from the others. The overview of significantly enriched or depleted proteins (Fig. 4c) shows time-dependent increases of significantly enriched proteins mainly on the surface of bare SWCNT-2 (without ecocorona), which is in agreement with the obtained PCAs (Fig. 4b). Such clear time-dependent alterations were not observed in the other treatments.

We have broken down the protein corona to individual proteins, which enabled us to identify the specific proteins responsible for the formation of the protein corona. A total of 119 proteins were reliably identified in at least three out of four replicates (see Supporting Information). Herein, the proteins forming the protein corona were investigated based on their Log2(FC) relative to their abundance in pure fish plasma. Thus, the top 10 most enriched proteins over all time points were identified for the different conditions, focusing on those that showed significant enrichment compared to pure fish plasma (Fig. 4e and 4f). In the presence of the ecocorona, we found Alpha chain, Vitellogenin B1 and B2 and CD11–1 on SWCNT-1, while these proteins were not detected on the bare SWCNT-1. For the SWCNT-2, in the presence of the ecocorona, we detected the proteins L-lactate dehydrogenase A chain, Tumor necrosis factor-3 alpha and Apolioprotein C1 a. These proteins were not detectable on the bare SWCNT-2. We found proteins that were part of the top 10 enriched proteins under several of the tested conditions as well as such that were unique for one condition (Fig. 4d). Transferrin a (Uniprot ID I6QXU6), which plays key roles in iron metabolism, was found in the list of top 10 enriched proteins under all conditions. Further proteins that were shared in at least three of the investigated conditions were serotransferrin (Uniprot ID B3GPN2), antithrombin III (Uniprot ID O42614), which inhibits blood coagulation, parvalbumin beta (Uniprot ID P02618), which plays a key role in calcium binding and is involved in calcium signaling, and gamma fibrinogen (Uniprot ID O42309), which functions in blood clotting.

Additionally, the top 10 lists of enriched proteins contained unique entries for all conditions. For instance, hemoglobin alpha (Uniprot ID M9V0L3) was unique for biocorona-SWCNT-1 (without ecocorona) and apolipoprotein Alb1 (Uniprot ID A0A076JYB9) was unique for biocorona-SWCNT-2. An alpha chain fragment (Uniprot ID A0A0U2SE40) and CD11–1 (Uniprot ID Q98TF1) were found to be unique for bio-ecocorona-SWCNT-1 and tumor necrosis factor-3 alpha (Uniprot ID Q7T2Q3) and apolipoprotein C I a (Uniprot ID X2EXL8) for bio-ecocorona-SWCNT-2.

4. Discussion

The topic of NM-biological corona is in its early stage with many analytical limitations. There is no validated protocol to determine the dynamics of corona formation on the surface of NMs. Ecotoxicologists and human toxicologists are currently attempting to unravel the impact

of a biological corona on the toxico-kinetic of NMs and their biological responses. Our results show that performing "injection" or neglecting the exposure pathway of NMs is a simplification of the reality for environmental risk assessment of NMs. The fit-for-purpose methods we describe here provide perspectives towards further mechanistically understanding of the processes underlying the dynamics of corona formation on the surface of DOM-coated NMs. We must emphasize that the uptake of DOM-coated NMs, in general, through e.g. fish digestive tract or gills, is not reported yet. This implies that DOM-coated NMs may not directly enter blood vessels and interact with plasma proteins. It is therefore required to understand the transformation of DOM-coated NMs before entering the blood and interacting with biological molecules.

The tested SWCNTs formed a highly unstable dispersion in water. This could be a result of strong van der Waals interactions between the tubes, which have been reported to be ~500 eV per μm of tube−tube contact (Girifalco et al., 2000; O'Connell et al., 2002). In a DOM suspension, the high free surface energy of the SWNCTs and the highly hydrophobic surface of the tubes (White et al., 2007) attracted DOM to the surface of the nanotubes. Considering the fact that DOM are ubiquitous materials in the aquatic environment, which is of a highly heterogeneous composition, it is inevitable that in the environment SWCNTs adsorb DOM on their surfaces. Moreover, DOM is rich in reactive groups such as hydroxyls, amines, thiols, and carboxylic acids that could provide sites for adsorption to the SWCNTs (Hyung et al., 2007). Formation of the DOM ecocorona on the surface of NMs changes the surface properties of the NMs, and consequently the bioavailability and the toxicity of the NMs (Lin et al., 2012). The mechanisms through which the DOM ecocorona changes the toxicity of the NMs is not clear.

In plasma, biomolecules adsorbed to the SWCNTs to form a biocorona. The ecocorona and the subsequently formed biocorona led to colloidal stabilization of the SWCNTs, which is in agreement with previous studies (Zeinabad et al., 2016) and could be attributed to the increased absolute value of the ζ-potential of the SWCNTs. In general, for NMs to reach colloidal stability, the ζ-potential should be at least $\sim$ −30 mV (Casals et al., 2010). We observed that after 5 min and 1 h of incubation, the ζ-potential of both biocorona-SWCNTs was above - 30 mV. Nevertheless, the SWCNTs showed a partial stability, which could result from steric effects induced by the biocorona (Gebauer et al., 2012; Gunawan et al., 2014).

The increase in the average thickness of the biocorona-SWCNT complexes over time was expected. In a previous study, an increase in the average thickness of a biocorona on the surface of 10 nm gold NM has been reported (up to 16 nm after 48 h incubation time), where the thickness was determined by measuring the hydrodynamic diameter over the incubation time (Casals et al., 2010).

Interestingly, we observed a thicker biocorona with a significantly higher amount of proteins attached to the surface of SWCNT-1 compared to SWCNT-2 at incubation times longer than 5 min. This indicates that when SWCNTs are incubated in plasma, biomolecules (proteins and other compounds) initially (< 5 min) occupy the surface of the SWCNTs regardless of the size of the tubes due to the high free surface energy of the nanotubes. However, by further evolution of the biocorona on the surface of SWCNTs and the decrease in the free surface energy, the size of the tubes could play a pronounced role in the further evolution of the biocorona. Due to the high-aspect-ratio of SWCNTs (Dutta et al., 2007), the biomolecules may align along the longitudinal axis to fit on the SWCNT surface (Monopoli et al., 2012). The variation in the aspect ratio or the absolute length of the SWCNTs could explain the differences observed in the amount of adsorbed biocorona from the plasma on the surface of the SWCNTs (Casals et al., 2010), as confirmed by our findings. The increase in the diameter of the biocorona-SWCNT complex may influence the cellular uptake of the SWCNTs by phagocytic cells, as reported for other types of NMs, such as polystyrene (Lesniak et al., 2010), and consequently their biological fate in an organism's body (Saptarshi et al., 2013).
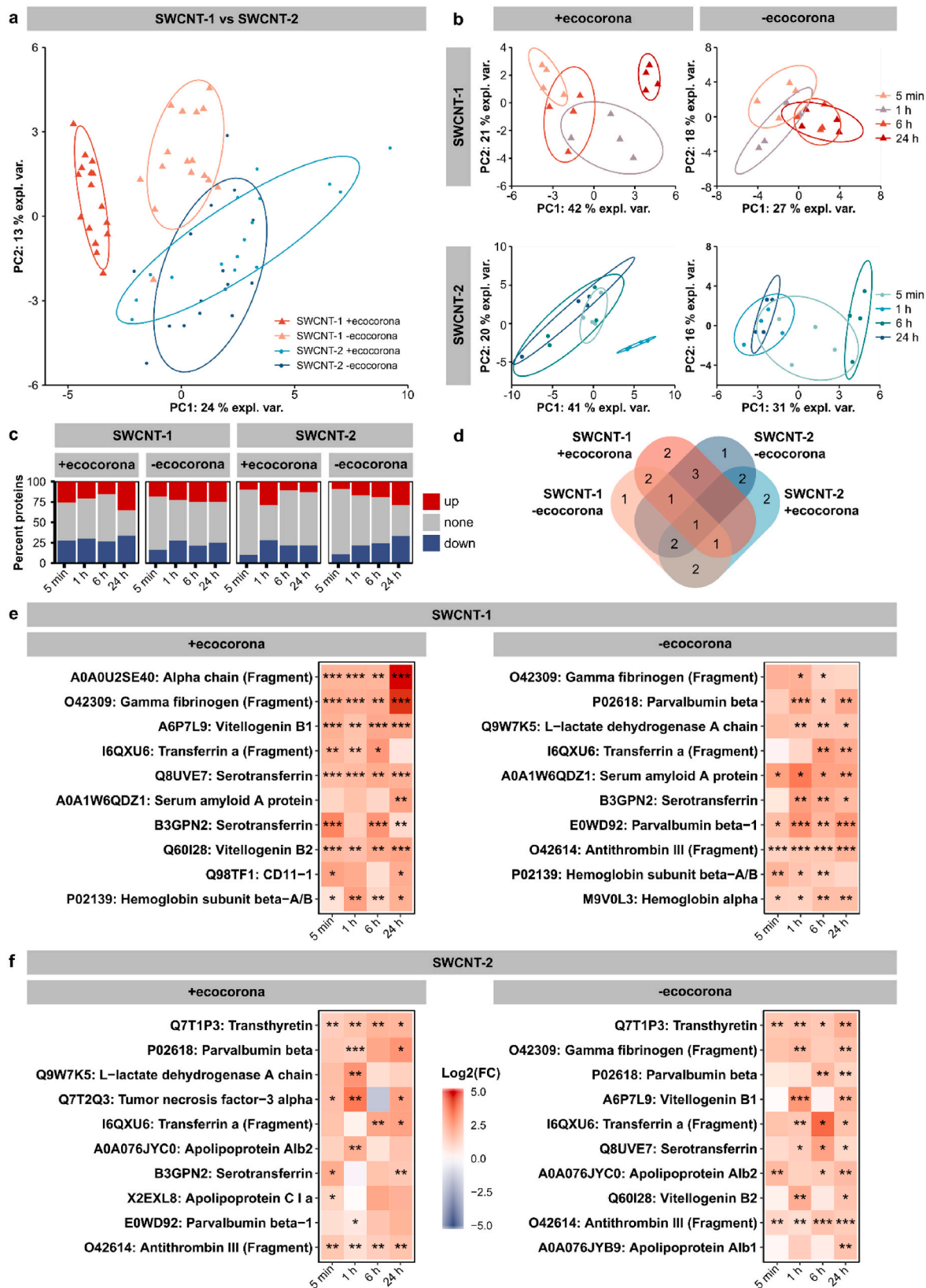
Fig. 4. Results of the Principle Component Analysis of obtained Log2(FCs) relative to pure fish plasma over all time points (a) and with separation of the time points (b). c) Summary of significantly (p.adj ≤ 0.05) enriched and depleted proteins upon incubation of pure fish plasma with the SWCNTs. d) Overlaps for the top 10 enriched proteins under the different conditions. e-f) show the Log2(FCs) and significances (p.adj ≤ 0.05: *; p.adj ≤ 0.01: **; p.adj ≤ 0.001: ***) of the top 10 most enriched proteins for SWCNT-1 and SWCNT-2, respectively.

Our findings show that the presence of an ecocorona dramatically influenced the interaction of biomolecules of plasma with SWCNTs. For example, the ζ-potential and the thickness of bio-ecocorona-SWCNTs changed significantly compared to biocorona-coated SWCNTs without an ecocorona. However, unlike for biocorona, the nanotube size did not influence the thickness of the bio-ecocorona on the surface of SWCNTs. These findings suggest that attachment of an ecocorona on NMs, which occurs inevitably when NMs enter the environment (Abdolahpur Monikh et al., 2018), may act as an environmental code that determines the further behavior of the NMs in biological systems. It has been previously shown that varying the surface chemistry of NMs [22] using a single surfactant (Kapralov et al., 2012) or protein (Maiorano et al., 2010; Oliveira et al., 2015) can affect the identity and quantity of proteins adsorbed on the NMs. In this study, we showed that the presence of an ecocorona affects the subsequent formation and evolution of a biocorona on the surface of SWCNTs.

Our finding further indicate that when DOM-coated SWCNTs enter the bloodstream, a fraction of the ecocorona is replaced by biomolecules over time due to the high affinity of the biomolecules to the surface of the SWCNTs compared to the ecocorona. However, the biocorona could not replace the entire ecocorona. This is of paramount importance for nanotoxicology because it implies that the prediction of the biological fate of NMs is difficult if they are taken up from the environment due to the limitless variations in the composition of DOM molecules from place to place and day to day, which may offer various identities to the surface of the NMs.

Our proteomics findings confirmed that the formation of a biocorona on SWCNTs is a size-dependent phenomenon because different protein compositions were determined on the surface of SWCNT-1 compared to SWCNT-2. The attachment of proteins to the surface of NMs depends in general on the affinity of the protein, the surface chemistry of the NM and the surface energy of the NM (Baimanov et al., 2019; Gunawan et al., 2014; Xia et al., 2011). However, time was not a significant influential factor on the evolution of protein corona on the surface of the SWCNTs. This suggests that protein exchange between the surface of the SWCNTs and the plasma may be a very fast process, as compared to the time scale of monitoring, and the equilibrium with regard to the composition of the protein corona could be reached in less than 5 min. This finding is consistent with previous modeling and empirical studies, which showed that the significant changes in the composition of a protein corona on the surface of NMs occur mostly in the early incubation period (Dell'Orco et al., 2010; Tenzer et al., 2013; Zhang et al., 2011).

When biological molecules, including proteins, immediately attach to the available surface of the SWCNTs, a rapid increase in the value of FCs is detectable. Further changes in the Log2(FCs) over time might not be observable due to the decreases in the surface energy and surface area, which are necessary for further adsorption of proteins (Casals et al., 2010). This may also lead to the formation of a loose protein corona, known as soft corona. We must mention that a typical method used to determine the protein corona composition is by extraction of all strongly adsorbed proteins from the surface of NMs into a single sample. However, because the protein corona is not at thermodynamic equilibrium (Monopoli et al., 2012), variation in the composition of the corona is inevitable, and observable to some extent, even between NMs of the same type and size (Lartigue et al., 2012). A soft corona can for example be easily detached from the surfaces upon sample handling and sample preparation (Casals et al., 2010; Tenzer et al., 2013), e.g., during separation of the corona from the SWCNTs. The observed time-dependent increase in the thickness of the biocorona could be related to adsorption of other biomolecules (Kapralov et al., 2012; Zeng et al., 2012) rather than only proteins. This finding suggests that consideration of the full biocorona can provide a more realistic picture of the biological fate of NMs. Nevertheless, most studies have aimed to bypass this process of understanding the entire biocorona to allow for simplicity (Monopoli et al., 2012).

The size of SWCNTs and the presence of a pre-attached ecocorona had an impact on the composition of the protein corona. Proteins have different binding capacities to SWCNTs, which may lead to competitive protein binding on the SWCNT surfaces (Ge et al., 2011). We demonstrated that transferrin, serotransferrin, antithrombin III, Parvalbumin beta gamma fibrinogen were shared between at least three of the treatments. A previous study also reported that transferrin, bovine serum albumin and bovine fibrinogen were predominantly able to bind to SWCNTs (Oliveira et al., 2015). It was reported that proteins with a higher number of hydrophobic amino acids on the surface have a high adsorption rate to SWCNTs (Ge et al., 2011). A considerable proportion of the amino acids on the human transferrin surface appear to be hydrophobic residues (MacGillivray et al., 1982), leading to formation of node-like complex aggregates onto the SWCNT surface (Ge et al., 2011). This may also be the case for carp transferrin. Bovine fibrinogen molecules are found to bind to SWCNTs non-uniformly due to the high number of hydrophobic amino acids and the large contact surfaces of the protein molecule to SWCNTs (Ge et al., 2011). Hydrophobic amino acids in the surface of antithrombin (Jairajpuri et al., 2003) and parvalbumin (Breiteneder and Mills, 2005) may also play a significant role in their interaction with the SWCNTs. Thus, it is also likely that the proportion of the amino acids in fish plasma proteins determined their affinity to SWCNTs.

The detected unique entries for all conditions suggest that the surface properties affect the affinities of individual proteins, in agreement with the literature (Ehrenberg et al., 2009; Koutsoukos et al., 1982). For example, surface functionalization of CNTs with carboxyl and polyvinylpyrrolidone led to association of unique proteins with the surface of the CNTs (Shannahan et al., 2013). In this study, we demonstrated that this can occur for DOM-coated SWCNTs as well, where the presence of an ecocorona on the surface of SWCNTs led to association of unique proteins with the SWCNTs. This suggests that when the surface of SWCNTs or other NMs is functionalized with different molecules of DOM, it is likely that each single NM obtains a unique protein corona, and consequently induces a unique set of biological fate and unique biological responses (Maiorano et al., 2010).

5. Conclusions

Formation of an ecocorona on the surface of SWCNTs after entering the environment significantly influences the formation and composition of a biocorona on the surface of the particles upon entering an organism. The biocorona may influence the biological fate of a nanotube, e.g. accumulation, biodistribution, and whether the nanotube remains in the body or is eliminated from it, which is of paramount importance for nanotoxicology. The presence of an ecocorona on the surface of SWCNTs controls the thickness, surface charge and the composition of the biocorona on the SWCNTs. The ecocorona offers a unique composition of a biocorona to each SWCNT. Although the formation of a biocorona is tube size-dependent, in the presence of an ecocorona on the surface of the tubes, size does not play a considerable role in the formation of a biocorona and its evolution on the SWCNTs. The results obtained suggest that the environment can modify SWCNTs and influence the formation of the biocorona when the nanotubes are taken up by organisms. Future studies might investigate how the ecocorona on NMs can influence the toxicity profile of the particles. This study can be the first building block for future studies to understand the mechanisms behind the influence of the ecocorona on the biological corona. We recommended future studies to focus on understanding the biological fate of CNT- bio-ecocorona in organisms' bodies.

Author contributions

F.A.M. conceptualized, supervised, wrote and reviewed the paper. F. A.M, L.C. perfumed the DOM labelling and measurements. F.A.M and D. A.L performed the incubation of SWCNTs with DOM and proteins. L.C.,

E.Z, and V·P cultured fish and extracted plasma from fish blood and contributed to editing the paper. F.A.M and L.C. extracted the proteins from SWCNTs. I·K, M.V.B and K·S performed the preparation of protein corona samples for LC-MS/MS, subsequent analyses using LC-MS/MS and editing the paper. F.A. M. and Z.G. Performed the TEM images. W.J., W.P. and M.V. contribute to the supervision and editing the paper.

Availability of data and materials

Ethics approval

All experiments were performed with the approval of the ethics committee of the Research Center of Aquaculture and Biodiversity of Hydrocenoses, the University of South Bohemia in Ceske Budejovice, Czech Republic (MSMT-6744/2018–4).

Consent for publication

All authors read and approved the final manuscript.

Declaration of Competing Interest

The authors declare no competing financial interests.

Acknowledgements

Appendix A. Supplementary data

Supplementary data to this article can be found online at https://doi.org/10.1016/j.impact.2021.100315.

References

Abdolahpur Monikh, F., Praetorius, A., Schmid, A., Kozin, P., Meisterjahn, B., Makarova, E., Hofmann, T., von der Kammer, F., 2018. Scientific rationale for the development of an OECD test guideline on engineered nanomaterial stability. NanoImpact 11, 42–50.

Albanese, A., Walkey, C.D., Olsen, J.B., Guo, H., Emili, A., Chan, W.C.W., 2014. Secreted biomolecules Alter the biological identity and cellular interactions of nanoparticles. ACS Nano 8, 5515–5526.

Arenas-Lago, D., Abdolahpur Monikh, F., Vijver, M.G., Peijnenburg, W.J.G.M., 2019. Dissolution and aggregation kinetics of zero valent copper nanoparticles in (simulated) natural surface waters: simultaneous effects of pH, NOM and ionic strength. Chemosphere 226, 841–850.

Baimanov, D., Cai, R., Chen, C., 2019. Understanding the chemical nature of nanoparticle–protein interactions. Bioconjug. Chem. 30, 1923–1937.

Bannuscher, A., Karkossa, I., Buhs, S., Nollau, P., Kettler, K., Balas, M., Dinischiotu, A., Hellack, B., Wiemann, M., Luch, A., von Bergen, M., Haase, A., Schubert, K., 2019. A multi-omics approach reveals mechanisms of nanomaterial toxicity and structure–activity relationships in alveolar macrophages. Nanotoxicology 1–15.

Breiteneder, H., Mills, E.N.C., 2005. Molecular properties of food allergens. J. Allergy Clin. Immunol. 115, 14–23.

Casals, E., Pfaller, T., Duschl, A., Oostingh, G.J., Puntes, V., 2010. Time evolution of the nanoparticle protein Corona. ACS Nano 4, 3623–3632.

Cedervall, T., Lynch, I., Foy, M., Berggård, T., Donnelly, S.C., Cagney, G., Linse, S., Dawson, K.A., 2007. Detailed identification of plasma proteins adsorbed on copolymer nanoparticles. Angew. Chem. Int. Ed. 46, 5754–5756.

Chen, R.J., Bangsaruntip, S., Drouvalakis, K.A., Wong Shi Kam, N., Shim, M., Li, Y., Kim, W., Utz, P.J., Dai, H., 2003. Noncovalent functionalization of carbon nanotubes for highly specific electronic biosensors. Proc. Natl. Acad. Sci. 100, 4984–4989.

Chetwynd, A.J., Lynch, I., 2020. The rise of the nanomaterial metabolite corona, and emergence of the complete corona. Environ. Sci.: Nano 7, 1041–1060.

De Volder, M.F.L., Tawfick, S.H., Baughman, R.H., Hart, A.J., 2013. Carbon nanotubes: present and future commercial applications. Science 339, 535–539.

Dell'Orco, D., Lundqvist, M., Oslakovic, C., Cedervall, T., Linse, S., 2010. Modeling the time evolution of the nanoparticle-protein Corona in a body fluid. PLoS One 5, e10949.

Du, T., Shi, G., Liu, F., Zhang, T., Chen, W., 2019. Sulfidation of Ag and ZnO Nanomaterials significantly affects protein Corona composition: implications for human exposure to environmentally aged Nanomaterials. Environ. Sci. Technol. 53, 14296–14307.

Dutta, D., Sundaram, S.K., Teeguarden, J.G., Riley, B.J., Fifield, L.S., Jacobs, J.M., Addleman, S.R., Kaysen, G.A., Moudgil, B.M., Weber, T.J., 2007. Adsorbed proteins influence the biological activity and molecular targeting of Nanomaterials. Toxicol. Sci. 100, 303–315.

Ehrenberg, M.S., Friedman, A.E., Finkelstein, J.N., Oberdörster, G., McGrath, J.L., 2009. The influence of protein adsorption on nanoparticle association with cultured endothelial cells. Biomaterials 30, 603–610.

Fadare, O.O., Wan, B., Liu, K., Yang, Y., Zhao, L., Guo, L.-H., 2020. Eco-corona vs protein corona: effects of humic substances on corona formation and nanoplastic particle toxicity in daphnia magna. Environ. Sci. Technol. 54 (13), 8001–8009.

Francia, V., Yang, K., Deville, S., Reker-Smit, C., Nelissen, I., Salvati, A., 2019. Corona composition can affect the mechanisms cells use to internalize nanoparticles. ACS Nano 13, 11107–11121.

Gasser, M., Rothen-Rutishauser, B., Krug, H.F., Gehr, P., Nelle, M., Yan, B., Wick, P., 2010. The adsorption of biomolecules to multi-walled carbon nanotubes is influenced by both pulmonary surfactant lipids and surface chemistry. J. Nanobiotechnol. 8, 31.

Ge, C., Du, J., Zhao, L., Wang, L., Liu, Y., Li, D., Yang, Y., Zhou, R., Zhao, Y., Chai, Z., Chen, C., 2011. Binding of blood proteins to carbon nanotubes reduces cytotoxicity. Proc. Natl. Acad. Sci. 108, 16968–16973.

Gebauer, J.S., Malissek, M., Simon, S., Knauer, S.K., Maskos, M., Stauber, R.H., Peukert, W., Treuel, L., 2012. Impact of the nanoparticle–protein Corona on colloidal stability and protein structure. Langmuir 28, 9673–9679.

Girifalco, L.A., Hodak, M., Lee, R.S., 2000. Carbon nanotubes, buckyballs, ropes, and a universal graphitic potential. Phys. Rev. B 62, 13104–13110.

Gunawan, C., Lim, M., Marquis, C.P., Amal, R., 2014. Nanoparticle–protein corona complexes govern the biological fates and functions of nanoparticles. J. Mater. Chem. B 2, 2060–2083.

Helbert, W., Chanzy, H., Husum, T.L., Schülein, M., Ernst, S., 2003. Fluorescent cellulose microfibrils as substrate for the detection of Cellulase activity. Biomacromolecules 4, 481–487.

Higgins, P., Dawson, J., Walters, M., 2011. Nanotubes reduce stroke damage. Nat. Nanotechnol. 6, 83–84.

Hughes, C.S., Moggridge, S., Muller, T., Sorensen, P.H., Morin, G.B., Krijgsveld, J., 2018. Single-pot, solid-phase-enhanced sample preparation for proteomics experiments. Nat. Protoc. 14, 68–85.

Hyung, H., Fortner, J.D., Hughes, J.B., Kim, J.-H., 2007. Natural organic matter stabilizes carbon nanotubes in the aqueous phase. Environ. Sci. Technol. 41, 179–184.

Jairajpuri, M.A., Lu, A.Q., Desai, U., Olson, S.T., Bjork, I., Bock, S.C., 2003. Antithrombin III phenylalanines 122 and 121 contribute to its high affinity for heparin and its conformational activation. J. Biol. Chem. 278, 15941–15950.

Javey, A., Guo, J., Wang, Q., Lundstrom, M., Dai, H., 2003. Ballistic carbon nanotube field-effect transistors. Nature 424, 654–657.

Kapralov, A.A., Feng, W.H., Amoscato, A.A., Yanamala, N., Balasubramanian, K., Winnica, D.E., Kisin, E.R., Kotchey, G.P., Gou, P., Sparvero, L.J., Ray, P., Mallampalli, R.K., Klein-Seetharaman, J., Fadeel, B., Star, A., Shvedova, A.A., Kagan, V.E., 2012. Adsorption of surfactant lipids by single-walled carbon nanotubes in mouse lung upon pharyngeal aspiration. ACS Nano 6, 4147–4156.

Karkossa, I., Bannuscher, A., Hellack, B., Bahl, A., Buhs, S., Nollau, P., Luch, A., Schubert, K., von Bergen, M., Haase, A., 2019. An in-depth multi-omics analysis in RLE-6TN rat alveolar epithelial cells allows for nanomaterial categorization. Particle and Fibre Toxicol. 16, 38.

Koutsoukos, P.G., Mumme-Young, C.A., Norde, W., Lyklema, J., 1982. Effect of the nature of the substrate on the adsorption of human plasma albumin. Colloids Surf. 5, 93–104.

Krahn, K.N., Bouten, C.V.C., van Tuijl, S., van Zandvoort, M.A.M.J., Merkx, M., 2006. Fluorescently labeled collagen binding proteins allow specific visualization of collagen in tissues and live cell culture. Anal. Biochem. 350, 177–185.

Kumar, A., Bicer, E.M., Morgan, A.B., Pfeffer, P.E., Monopoli, M., Dawson, K.A., Eriksson, J., Edwards, K., Lynham, S., Arno, M., Behndig, A.F., Blomberg, A., Somers, G., Hassall, D., Dailey, L.A., Forbes, B., Mudway, I.S., 2016. Enrichment of immunoregulatory proteins in the biomolecular corona of nanoparticles within human respiratory tract lining fluid. Nanomedicine 12, 1033–1043.

Lacerda, L., Bianco, A., Prato, M., Kostarelos, K., 2006. Carbon nanotubes as nanomedicines: from toxicology to pharmacology. Adv. Drug Deliv. Rev. 58, 1460–1470.

Lartigue, L., Wilhelm, C., Servais, J., Factor, C., Dencausse, A., Bacri, J.-C., Luciani, N., Gazeau, F., 2012. Nanomagnetic sensing of blood plasma protein interactions with Iron oxide nanoparticles: impact on macrophage uptake. ACS Nano 6, 2665–2678.

Lesniak, A., Campbell, A., Monopoli, M.P., Lynch, I., Salvati, A., Dawson, K.A., 2010. Serum heat inactivation affects protein corona composition and nanoparticle uptake. Biomaterials 31, 9511–9518.

Lin, D., Ji, J., Long, Z., Yang, K., Wu, F., 2012. The influence of dissolved and surface-bound humic acid on the toxicity of TiO2 nanoparticles to Chlorella sp. Water Res. 46, 4477–4487.

Lundqvist, M., Stigler, J., Cedervall, T., Berggård, T., Flanagan, M.B., Lynch, I., Elia, G., Dawson, K., 2011. The evolution of the protein Corona around nanoparticles: a test study. ACS Nano 5, 7503–7509.

Lynch, I., Dawson, K.A., 2008. Protein-nanoparticle interactions. Nano Today 3, 40–47.

Lynch, I., Cedervall, T., Lundqvist, M., Cabaleiro-Lago, C., Linse, S., Dawson, K.A., 2007. The nanoparticle–protein complex as a biological entity; a complex fluids and surface science challenge for the 21st century. Adv. Colloid Interf. Sci. 134-135, 167–174.

MacGillivray, R.T., Mendez, E., Sinha, S.K., Sutton, M.R., Lineback-Zins, J., Brew, K., 1982. The complete amino acid sequence of human serum transferrin. Proc. Natl. Acad. Sci. 79, 2504–2508.

Maiorano, G., Sabella, S., Sorce, B., Brunetti, V., Malvindi, M.A., Cingolani, R., Pompa, P. P., 2010. Effects of cell culture media on the dynamic formation of protein−nanoparticle complexes and influence on the cellular response. ACS Nano 4, 7481–7491.

Monopoli, M.P., Walczyk, D., Campbell, A., Elia, G., Lynch, I., Baldelli Bombelli, F., Dawson, K.A., 2011. Physical−chemical aspects of protein Corona: relevance to in vitro and in vivo biological impacts of nanoparticles. J. Am. Chem. Soc. 133, 2525–2534.

Monopoli, M.P., Åberg, C., Salvati, A., Dawson, K.A., 2012. Biomolecular coronas provide the biological identity of nanosized materials. Nat. Nanotechnol. 7, 779–786.

Mu, Q., Liu, W., Xing, Y., Zhou, H., Li, Z., Zhang, Y., Ji, L., Wang, F., Si, Z., Zhang, B., Yan, B., 2008. Protein binding by functionalized multiwalled carbon nanotubes is governed by the surface chemistry of both parties and the nanotube diameter. J. Phys. Chem. C 112, 3300–3307.

Nel, A.E., Mädler, L., Velegol, D., Xia, T., Hoek, E.M.V., Somasundaran, P., Klaessig, F., Castranova, V., Thompson, M., 2009. Understanding biophysicochemical interactions at the nano–bio interface. Nat. Mater. 8, 543–557.

O'Connell, M.J., Bachilo, S.M., Huffman, C.B., Moore, V.C., Strano, M.S., Haroz, E.H., Rialon, K.L., Boul, P.J., Noon, W.H., Kittrell, C., Ma, J., Hauge, R.H., Weisman, R.B., Smalley, R.E., 2002. Band gap fluorescence from individual single-walled carbon nanotubes. Science 297, 593–596.

Oliveira, S.F., Bisker, G., Bakh, N.A., Gibbs, S.L., Landry, M.P., Strano, M.S., 2015. Protein functionalized carbon nanomaterials for biomedical applications. Carbon 95, 767–779.

Pantarotto, D., Briand, J.-P., Prato, M., Bianco, A., 2004. Translocation of bioactive peptides across cell membranes by carbon nanotubes. Chem. Commun. 16–17.

Perez-Riverol, Y., Csordas, A., Bai, J., Bernal-Llinares, M., Hewapathirana, S., Kundu, D. J., Inuganti, A., Griss, J., Mayer, G., Eisenacher, M., Pérez, E., Uszkoreit, J., Pfeuffer, J., Sachsenberg, T., Yilmaz, S., Tiwary, S., Cox, J., Audain, E., Walzer, M., Jarnuczak, A.F., Ternent, T., Brazma, A., Vizcaíno, J.A., 2019. The PRIDE database and related tools and resources in 2019: improving support for quantification data. Nucleic Acids Res. 47 (D1), D442–D450 (PubMed ID: 30395289).

Perng, W., Palui, G., Wang, W., Mattoussi, H., 2019. Elucidating the role of surface coating in the promotion or prevention of protein Corona around quantum dots. Bioconjug. Chem. 30, 2469–2480.

Saptarshi, S.R., Duschl, A., Lopata, A.L., 2013. Interaction of nanoparticles with proteins: relation to bio-reactivity of the nanoparticle. J. Nanobiotechnol. 11, 26.

Shannahan, J.H., Brown, J.M., Chen, R., Ke, P.C., Lai, X., Mitra, S., Witzmann, F.A., 2013. Comparison of nanotube–protein Corona composition in cell culture media. Small 9, 2171–2181.

Simon, J., Muller, J., Ghazaryan, A., Morsbach, S., Mailander, V., Landfester, K., 2018. Protein denaturation caused by heat inactivation detrimentally affects biomolecular corona formation and cellular uptake. Nanoscale 10, 21096–21105.

Tenzer, S., Docter, D., Kuharev, J., Musyanovych, A., Fetz, V., Hecht, R., Schlenk, F., Fischer, D., Kiouptsi, K., Reinhardt, C., Landfester, K., Schild, H., Maskos, M., Knauer, S.K., Stauber, R.H., 2013. Rapid formation of plasma protein corona critically affects nanoparticle pathophysiology. Nat. Nanotechnol. 8, 772–781.

Thakare, V.S., Das, M., Jain, A.K., Patil, S., Jain, S., 2010. Carbon nanotubes in cancer theragnosis. Nanomedicine 5, 1277–1301.

White, B., Banerjee, S., O'Brien, S., Turro, N.J., Herman, I.P., 2007. Zeta-potential measurements of surfactant-wrapped individual single-walled carbon nanotubes. J. Phys. Chem. C 111, 13684–13690.

Xia, X.R., Monteiro-Riviere, N.A., Mathur, S., Song, X., Xiao, L., Oldenberg, S.J., Fadeel, B., Riviere, J.E., 2011. Mapping the surface adsorption forces of Nanomaterials in biological systems. ACS Nano 5, 9074–9081.

Xu, L.N., Xu, M., Wang, R.X., Yin, Y.G., Lynch, I., Liu, S.J., 2020. The crucial role of environmental coronas in determining the biological effects of engineered nanomaterials. Small 16.

Yang, K., Xing, B., 2009. Adsorption of fulvic acid by carbon nanotubes from water. Environ. Pollut. 157, 1095–1100.

Zeinabad, H.A., Zarrabian, A., Saboury, A.A., Alizadeh, A.M., Falahati, M., 2016. Interaction of single and multi wall carbon nanotubes with the biological systems: tau protein and PC12 cells as targets. Sci. Rep. 6, 26508.

Zeng, Z., Patel, J., Lee, S.-H., McCallum, M., Tyagi, A., Yan, M., Shea, K.J., 2012. Synthetic polymer nanoparticle–polysaccharide interactions: a systematic study. J. Am. Chem. Soc. 134, 2681–2690.

Zhang, H., Burnum, K.E., Luna, M.L., Petritis, B.O., Kim, J.-S., Qian, W.-J., Moore, R.J., Heredia-Langner, A., Webb-Robertson, B.-J.M., Thrall, B.D., Camp II, D.G., Smith, R. D., Pounds, J.G., Liu, T., 2011. Quantitative proteomics analysis of adsorbed plasma proteins classifies nanoparticles with different surface properties and size. PROTEOMICS 11, 4569–4577.